Seismic Velocity Variation within the Footwall of an Oceanic Core Complex – Atlantis Massif, Mid-Atlantic Ridge 30°N

Ashlee S. Henig, Donna K. Blackman, Alistair J. Harding, Graham M. Kent, Juan-Pablo Canales[1]
Scripps Institution of Oceanography USA
[1] Woods Hole Oceanographic Institution USA

Abstract

The Atlantis Massif, an oceanic core complex (OCC) at 30ºN on the Mid-Atlantic Ridge, is hypothesized to have formed via long-lived slip on a detachment fault. Due to unroofing that results from this sustained slip, the domal core of the OCC is predicted to comprise lower crustal and/or upper mantle rock. Seafloor mapping and deep drilling confirm that this is the case in local areas, and regional geophysical mapping allows us to extend these groundtruth data to infer the broader lithospheric architecture. New results for a multichannel seismic (MCS) line across the Southern Ridge of the massif motivate this report. Our findings require an important update to previously-published interpretations of the structure of this domal core: seismic velocity models indicate that a gabbroic body similar to that drilled in the Central Dome likely also exists in at least the eastern portion of the Southern Ridge.

Introduction

The formation of oceanic core complexes represents a style of rifting and accretion that occurs episodically at a variety of spreading centers (ranging from intermediate to ultra-slow spreading rates) as changes in the balance of magmatic and tectonic activity take place along the ridge. Recent models predict that a threshold percentage of 30-50% magmatic accretion versus tectonic extension is conducive to the development of long-lived detachment faults and the formation of OCCs during the exhumation of the footwall (Tucholke et al., 2008). The seismic structure of the footwall to the detachment fault controlling the formation of an OCC can document variability associated with the distribution of mafic (magmatic) versus altered ultramafic (tectonically extended, fractured) lithosphere within the OCC structure.

The domal core of the Atlantis Massif at 30°N on the Mid-Atlantic Ridge is comprised of two main structural components, the Southern Ridge and the Central Dome (Figure 1). The Southern Ridge of the massif, located adjacent to the Atlantis transform fault, rises to a topographic peak about 760 meters below the sea surface, just below which occurs the serpentinite-hosted Lost City Hydrothermal vent field (Kelley et al., 2001; 2005; Früh-Green et al., 2003). Mapping and sampling of bedrock exposed along mass wasting scars at the Southern Ridge have returned a combination of serpentinites, gabbros, and few basalts (Blackman et al., 2002; Karson et al., 2006). The deeper Central Dome is adjacent and morphologically continuous with the north side of the Southern Ridge. Spreading-parallel corrugations are visible on the surface of both domal highs and juxtaposed to the Central Dome, a narrow block of volcanics sits atop the eastern portion and is probably a remnant of the detachment fault hanging wall or rider blocks to the footwall (Blackman et al., 1998; 2002). Drilling at Integrated Ocean Drilling Program (IODP) Hole U1309D on the southern Central Dome recovered a 1.4 km, nearly continuous gabbroic sequence (Blackman et al., 2006). This OCC is similar to others with comparable data coverage, with seafloor samples returning a ratio of about

70% serpentinized peridotite and 30% gabbro whereas deep drilling recovers dominantly gabbro (Ildefonse et al., 2007; Dick et al., 2008).

Seismic refraction analyses of the domal core of Atlantis Massif (Canales et al., 2008; Collins et al., 2009) reveal a heterogeneous structure in the upper 0.5-1.5 km, with large P-wave velocity gradients at lateral scales of less than 1 km. Canales et al. (2008) use refracted arrivals picked from standard MCS shot gathers along Line 10 and invert these data to obtain a velocity model where shallow, high-velocity material (> 4.2 km/s) and large vertical velocity gradients (> 3 s^{-1}, Figure 2) occur beneath the eastern slope of the Central Dome. Shallow velocity less than 3.4 km/s and low vertical gradients (~1 s^{-1}) occur immediately beneath the western slope of the Central Dome. Similar analysis of Line 4 shows intermediate P-wave velocities and vertical gradients where this along-strike profile crossed the Southern Ridge, in the vicinity of its central peak (Figure 1). Velocity structure for Line 9 crossing the Southern Ridge in the dip direction was not considered in prior studies.

Data Analysis

MCS data collected in 2001 (Canales et al., 2004) are again employed in our study, but here we emphasize more detailed structure in the uppermost approximately one kilometer of structure. MCS data is advantageous over more conventional on-bottom seismic (OBS) datasets due to the multiplicity and even spatial distribution of the ray coverage. The Synthetic On-Bottom Experiment (SOBE) method used to process the data downward continues the shots and receivers to a depth just above the seafloor (Harding et al., 2007; Henig et al., 2008). The SOBE method overcomes one of the disadvantages of surface sources and receivers characteristic of MCS data by unmasking the shallowest turning rays covered by the water wave in areas of deep topography. This exposes more of the first refracted arrival in the shot gathers, allowing for the picking of refracted arrivals recorded on the streamer at very-near offset (300-2000 m range). The SOBE method provides constraints from rays turning in the upper few hundred meters, which were unavailable when standard shot gathers were analyzed by Canales et al., 2008. Improved models of the upper few hundred meters of the section enables greater confidence in the deeper (400-1500 m) structure obtained in the velocity model inversion.

Following the method of Van Avendonk (Van Avendonk et al., 2004), velocity structure of the massif is modeled by inverting the first refracted arrival time picks. The models are updated by minimizing the misfit between the predicted times and the picked times in a least squares sense. The initial result shown here for Line 9 (Figure 2a) represents both a good overall fit to the data, with χ^2 close to 1, and a good fit within each portion of the Line (ie. western slope, central area, and eastern slope). While additional tests of the effect of specific inversion parameters will affect details, the main result for Line 9 that we emphasize here is robust. Application of this method to Lines 10 (Blackman et al., 2009) and 4 (Henig et al., 2008) produce results that are in general agreement with the results of Canales et al. (2008; Figure 1) indicating that our implementation of downward continuation and inversion is robust.

The most obvious feature in our results for Line 9 (Figure 2a) is a large high-velocity body beneath the eastern half of the Southern Ridge. Velocities greater than 5km/s occur within the upper 200 meters and values greater than 6.2 km/s are reached within 500 meters of the seafloor (Figure 2b). Figure 2b shows that the velocities in this region are similar to the in situ velocities recorded in the drill hole U1309D on the Central Dome. This structure extends about 5 km in the ridge-perpendicular direction (1

to -4 km in model, Figure 2a). In contrast to the east, a noticeable thin low-velocity layer caps the western two-thirds of the Southern Ridge along Line 9. This layer extends laterally about 9 km (-2 to -11 km, Figure 2a) and has velocities of 2-3 km/s extending 100-400 meters below the surface (Figure 2b). Away from the high-velocity body and the low-velocity cap layer, model velocities are generally between 4 and 5.5 km/s.

With such a large range of velocities modeled in such a shallow depth range, there are high vertical velocity gradients and strong lateral heterogeneities along Line 9. The eastern high-velocity body has vertical gradients greater than 3.33 s^{-1}. The western portion has shallow gradients as high as 3 s^{-1} in the transition from the low-velocity cap to velocities >5 km/s at 1 km depth. Whereas the coverage of Canales et al. (2008) highlighted heterogeneity between the central and southern domes of Atlantis Massif, here we find additional heterogeneity within the Southern Ridge that is of comparable scale. The eastern portion of Line 9 is similar in velocity structure to that beneath the eastern slope of Line 10 and beneath the Central Dome where Line 4 crosses it.

Discussion

The velocity structure within the Atlantis Massif supports previous hypotheses regarding the formation of OCCs and their internal structure. The high-velocity body(ies) in Lines 4, 9, and 10 is(are) interpreted as a large mafic intrusion(s) surrounded by lower density material that is composed of shallower crustal rocks or highly serpentinized peridotite. This is consistent with gravity analysis that shows a positive gravity anomaly in the central/southeastern region of Line 9 (Blackman et al., 2008). If the rock surrounding the body is serpentinized peridotite, this velocity distribution supports the plum-pudding model of OCC formation (Escartin et al., 2003; Ildefonse et al., 2007) where mafic material is episodically injected into serpentinized mantle material that is exposed and altered by the exhumation of the footwall. The location of this intrusive body at the flank of the OCC closest to the ridge and the termination of the detachment also supports the increased-melt OCC extinction model previously proposed by Tucholke et al., 2008.

The low velocities in the upper few hundred meters of structure on the western side of the massif probably represent strongly fractured, permeable, and serpentinized peridotite. The observed velocity structure is indicative of prolonged weathering with increased distance from the ridge. Differences in the mechanical properties of rocks between the western and eastern portion of Line 9 such as crustal versus mantle composition, permeability versus impermeability, or susceptibility versus resistance to chemical alteration, might lead to such a velocity distribution within the OCC.

Ongoing Work

Downward continued MCS refraction velocity models in the upper ~1.5 km of the Atlantis Massif continue to reveal new seismic structure that indicate important geologic features of this oceanic core complex. Our ongoing work includes processing and analysis of the complete set of MCS lines (Figure 1a) at this OCC using the SOBE downward continuation technique. Velocity models along all of the along- and across-strike profiles will document the scale of variability within the upper lithosphere, providing for the first time a more comprehensive, 3-dimensional view into the OCC.

References

Blackman, D.K., Cann, J.R., Janssen, B. and Smith, D.K., 1998. Origin of extensional core complexes: Evidence from the Mid-Atlantic Ridge at Atlantis Fracture Zone. J. Geophys. Res., 103: 21315-21333.

Blackman, D.K., Karson, J.A., Kelley, D.S., Cann, J.R., Früh-Green, G.L., Gee, J.S., Hurst, S.D., John, B.E., Morgan, J., Nooner, S.L., Ross, D.K., Schroeder, T.J. and Williams, E.A., 2002. Geology of the Atlantis Massif (Mid-Atlantic Ridge, 30 degrees N): Implications for the evolution of an ultramafic oceanic core complex. Marine Geophys. Res., 23: 443-469.

Blackman, D.K., Ildefonse, B., John, B.E., Ohara, Y., Miller, D.J., MacLeod, C.J., and the Expedition 304/305 Scientists, 2006. Proc. IODP, 304/305: College Station TX (Integrated Ocean Drilling Program Management International, Inc.). doi:10.2204/iodp.proc.304305.

Blackman, D.K., Canales J.P., Harding, A.J., in press, 2009. Geophysical Signatures of Oceanic Core Complexes. Geophysical Journal International, in press.

Canales, J.P., Tucholke, B.E., and Collins, J.A., 2004. Seismic reflection imaging of an oceanic detachment fault: Atlantis megamullion (Mid-Atlantic Ridge, 30°10′ N). Earth Planet. Sci. Lett., 222:543–560.

Canales, J.P., Tucholke, B., Xu, M., Collins J.A. and DuBois, D.L., 2008. Seismic evidence for large-scale compositional heterogeneity of oceanic core complexes. Geochem. Geophys. Geosyst., 9: 10.1029/2008GC002009.

Collins, J. A., Blackman, D. K., Harris, A., Carlson, R. L, 2009. Seismic and drilling constrains on velocity structure and reflectivity near IODP Hole U1309D on the central dome of Altantis Massif, Mid-Atlantic Ridge 30°N, Geochem. Geophys. Geosyst., 10: 10.1029/2008GC002121.

Dick, H.J.B., Tivey, M.A., & Tucholke, B.E., 2008. Plutonic foundation of a slow-spreading ridge segment: the oceanic core complex at Kane Megamullion, 23°30'N, 45°20'W, Geochemisty, Geophysics, Geosystems, 9: 10.1029/2007GC001645.

Escartin, J., Mével, C., MacLeod, C.J. and McCaig, A.M., 2003. Constraints on deformation conditions and the origin of oceanic detachments: The Mid-Atlantic Ridge core complex at 15. Geochem. Geophys. Geosyst., 4: 10.1029/2002GC000472.

Früh-Green, G.L., Kelley, D.S., Bernasconi, S.M., Karson, J.A., Ludwig, K.A., Butterfield, D.A., Boschi, C. & Proskurowski, G., 2003. 30,000 years of hydrothermal activity at the Lost City vent field, Science, 301**,** 495-498.

Harding, A.J., Kent, G.M., Blackman, D.K., Singh, S. & Canales, J.P., 2007. A New Method for MCS Refraction DataAnalysis of the Uppermost Section at a Mid-Atlantic Ridge Core Complex, Eos Trans. AGU, 88(52)**,** Abstract S12A-03.

Henig, A.S., Blackman, D.K., Harding, A.J., Kent, G.M., & Canales, J.P., 2008. Additional constraints on the shallow seismic velocity structure of the Atlantis Massif oceanic core complex, AGU Fall Meeting**,** Abstract T43B-2016.

Ildefonse, B., Blackman, D.K., John, B.E., Ohara, Y., Miller, D.J., MacLeod, C.J., IODP Expeditions 304/305 Science Party, 2007. Oceanic core complexes and crustal accretion at slow-spreading ridges, Geology 35, 623-626.

Karson, J. A., Früh-Green, G. L., Kelley, D. S., Williams, E. A., Yoerger, D. R., Jakuba, M, 2006. Detachment shear zone of the Atlantis Massif core complex, Mid-Atlantic Ridge, 30°N, Geochem. Geophys. Geosyst., 7: 10.1029/2005GC001109.

Kelley, D.S., Karson, J.A., Blackman, D.K., Früh-Green, G.L., Butterfield, D.A., Lilley, M.D., Olson, E.J., Schrenk, M.O., Roe, K.K., Lebon, G.T. and Rivizzigno, P., 2001. An off-axis hydrothermal vent field near the Mid-Atlantic Ridge at 30 degrees N. Nature, 412: 145-149.

Kelley, D.S., et al., 2005. A Serpentinite-Hosted Ecosystem: The Lost City Hydrothermal Field, Science, 307**,** 1428.

Tucholke, B., Behn, M.D., Buck, W.R., Lin, J., 2008. Role of melt supply in oceanic detachment faulting and formation of megamullions, Geology, 36, 455-458.

Van Avendonk, H.J.A., Shillington, D.J., Holbrook, W.S. and Hornback, M.J., 2004. Inferring crustal structure in the Aleutian island arc from a sparse wide-angle seismic data set. Geochem. Geophys. Geosyst., 5: 10.1029/2003GC000664.

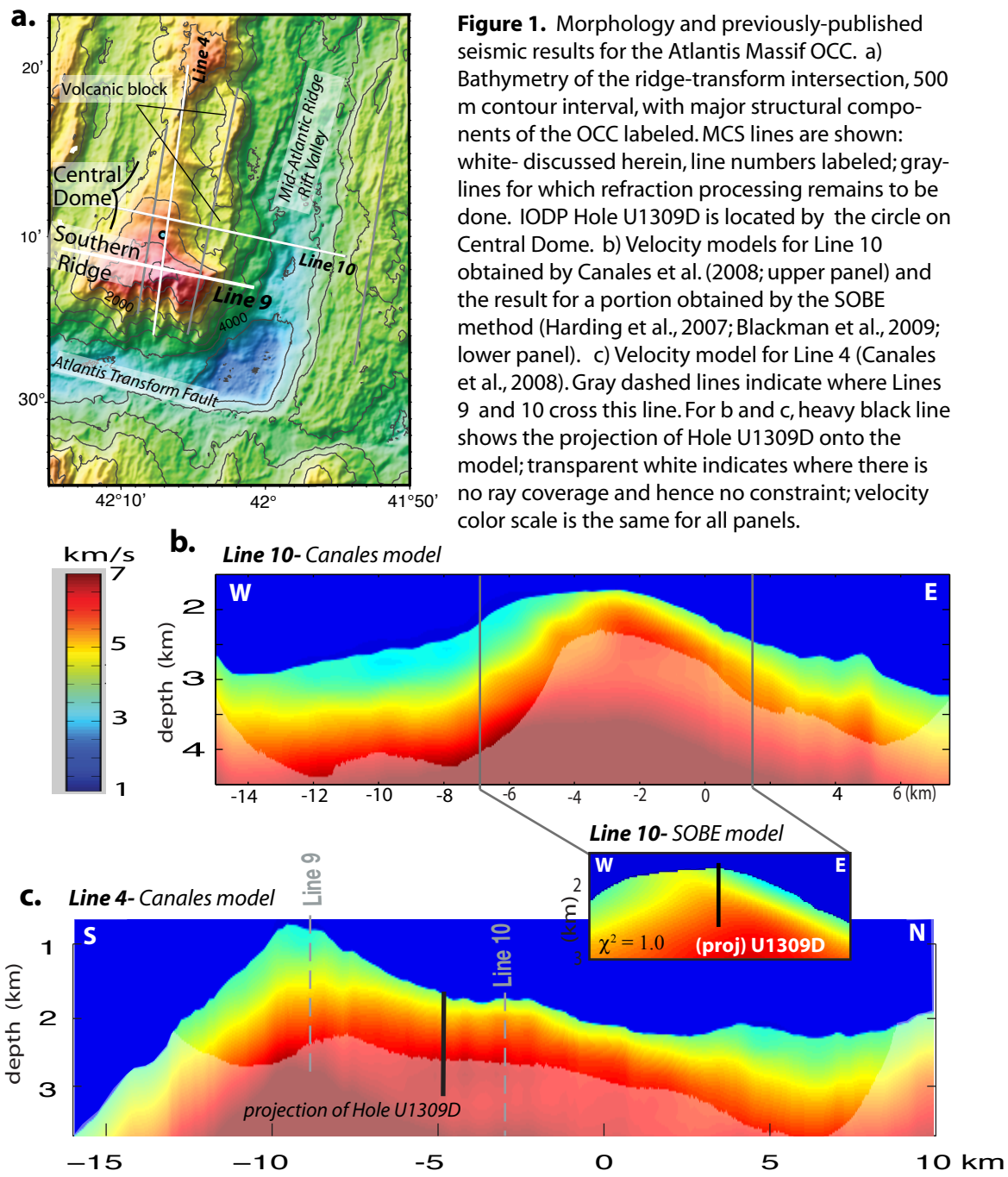

Figure 1. Morphology and previously-published seismic results for the Atlantis Massif OCC. a) Bathymetry of the ridge-transform intersection, 500 m contour interval, with major structural components of the OCC labeled. MCS lines are shown: white- discussed herein, line numbers labeled; gray- lines for which refraction processing remains to be done. IODP Hole U1309D is located by the circle on Central Dome. b) Velocity models for Line 10 obtained by Canales et al. (2008; upper panel) and the result for a portion obtained by the SOBE method (Harding et al., 2007; Blackman et al., 2009; lower panel). c) Velocity model for Line 4 (Canales et al., 2008). Gray dashed lines indicate where Lines 9 and 10 cross this line. For b and c, heavy black line shows the projection of Hole U1309D onto the model; transparent white indicates where there is no ray coverage and hence no constraint; velocity color scale is the same for all panels.

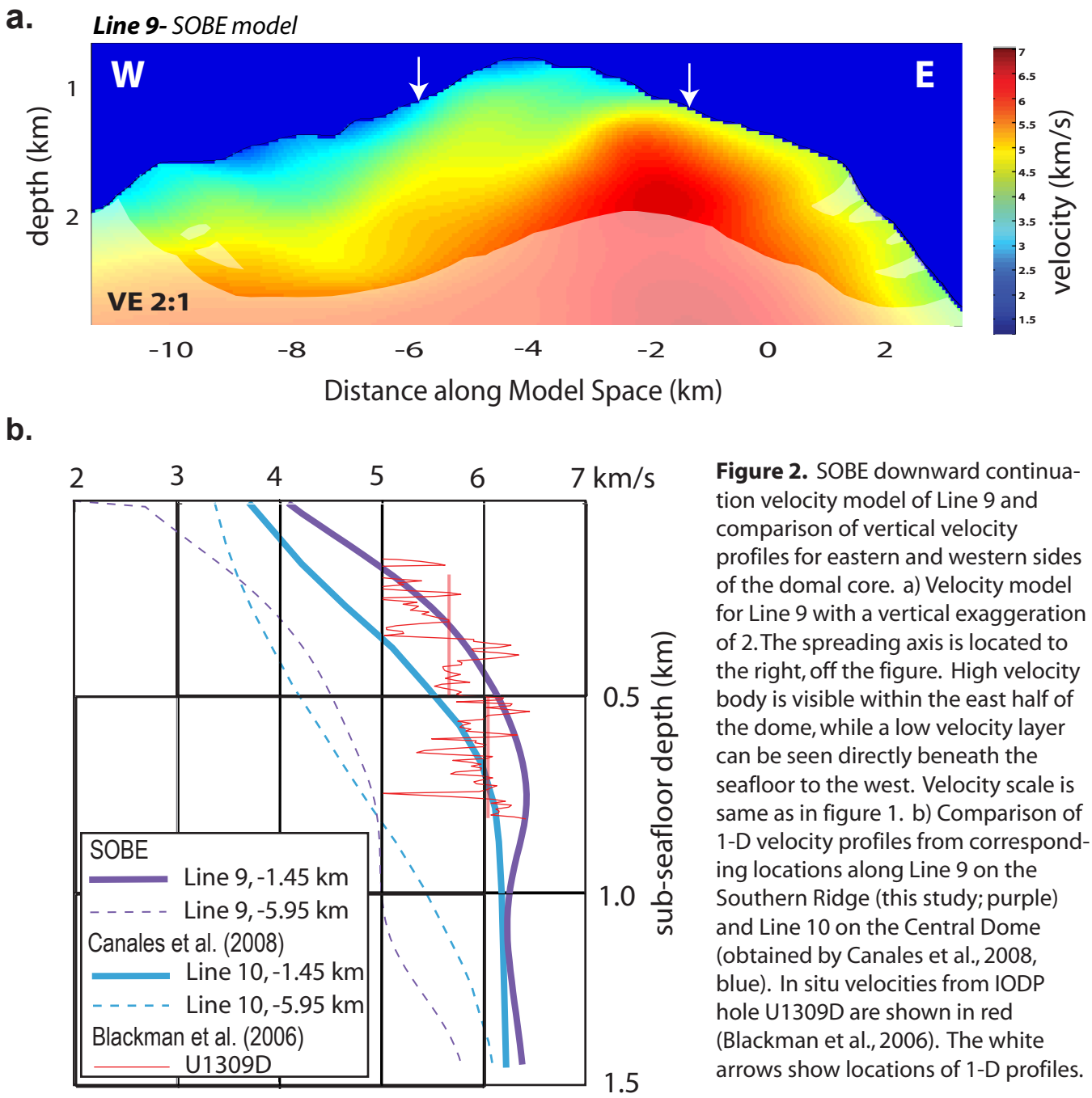

Figure 2. SOBE downward continuation velocity model of Line 9 and comparison of vertical velocity profiles for eastern and western sides of the domal core. a) Velocity model for Line 9 with a vertical exaggeration of 2. The spreading axis is located to the right, off the figure. High velocity body is visible within the east half of the dome, while a low velocity layer can be seen directly beneath the seafloor to the west. Velocity scale is same as in figure 1. b) Comparison of 1-D velocity profiles from corresponding locations along Line 9 on the Southern Ridge (this study; purple) and Line 10 on the Central Dome (obtained by Canales et al., 2008, blue). In situ velocities from IODP hole U1309D are shown in red (Blackman et al., 2006). The white arrows show locations of 1-D profiles.